

An Optimal Iterative Learning Control Approach for Linear Systems with Nonuniform Trial Lengths under Input Constraints

Zhihe Zhuang, Hongfeng Tao, Yiyang Chen, Vladimir Stojanovic, and Wojciech Paszke

Abstract—In practical applications of iterative learning control (ILC), the repetitive process may end up early by accident during the performance improvement along the trial axis, which yields the nonuniform trial length problem. For such practical systems, input signals are usually constrained because of some certain physical limitations. This paper proposes an optimal ILC algorithm for linear time-invariant multiple-input multiple-output (MIMO) systems with nonuniform trial lengths under input constraints. The optimal ILC framework is specifically modified for the nonuniform trial length problem, where the primal-dual interior point method is introduced to deal with the input constraints. Hence, the constraint handling capability are improved compared with the conventional counterparts for nonuniform trial lengths. Also, the monotonic convergence property of the proposed optimal ILC algorithm is obtained in the sense of mathematical expectation. Finally, the effectiveness of the proposed algorithm is verified on the numerical simulation of a mobile robot.

Index Terms—Iterative learning control (ILC), nonuniform trial length, input constraint, primal-dual interior point method.

I. INTRODUCTION

ITERATIVE learning control (ILC) is an effective approach that uses previous experiment data to handle the repetitive control processes, including chemical batch processing [1], [2], industrial robotic systems [3], robotic-assisted biomedical systems [4], networked stochastic systems [5], etc. Different from traditional control methodologies, ILC improves the tracking performance for repetitive signals by learning from

the historical information. Therefore, it is required that each trial operates over a finite time interval. More precisely, ILC employs the stored input and tracking error information from previous trials or even the current trial to update the input signal of next trial. Moreover, ILC is an open-loop control and usually has no feedback mechanism to respond to unanticipated, non-repeating disturbances [6]. More information can be obtained through surveys on ILC including [7]–[9].

In practical industrial processes, the classic postulate that each trial length must be identical cannot be always satisfied [10]. For instance, ILC can be used in functional electrical stimulation (FES) to help stroke patients who suffer from foot drop due to the repetitiveness of foot motion. However, FES should be applied at least before the initial contact between the foot and ground was detected for safety reasons, which thus leads to nonuniform trial length problem [11]. Another instance occurs in a gantry crane with output constraints [12]. Because the gantry crane cannot operate beyond a region restricted by some obstacles around, the duration of tracking is going to be nonidentical when using ILC schemes. In practice, obstacles may exist around the desired trajectory more or less when ILC is utilized to perform the trajectory tracking task, so the nonuniform trial length problem may be attributed to the output constraints. A further simulation example will be discussed in section V.

Due to generality of the nonuniform trial length problem, plenty of research has been conducted specifically. The main schemes to handle this problem concentrate on the enhancement of learning efficiency, such as [13]–[19]. However, different forms of methods lead to different control performance. Methods using traditional P-type ILC implementation such as [13]–[15], are a kind of lazy pattern, which means lower speed of convergence and poorer robustness to the randomness of nonuniform trial lengths. In [16]–[19], the iteration average operator was introduced to improve the utilization of historical information, while the performance may become poorer as the number of iteration increases, because the average operator may weaken the effect of the instant learning. Besides, a more effective method that uses the most recent existing trial information was proposed in [20], where the current time instant only benefits from the most recent existing trial information correspondingly. In contrast to simple zero compensation mechanism, an auxiliary model was employed to estimate the predictive outputs when the trial ends suddenly, which gives another direction to solve the nonuniform trial length problem [21]. However, the aforementioned research only focuses on

This work was supported in part by the National Natural Science Foundation of China under Grant 61773181, Grant 61203092 and Grant 62103293, in part by the 111 Project under Grant B12018, in part by the Fundamental Research Funds for the Central Universities under Grant JUSRP51733B, in part by the Serbian Ministry of Education, Science and Technological Development under Grant 451-03-9/2021-14/200108, in part by the National Science Centre in Poland under Grant 2020/39/B/ST7/01487, in part by the Natural Science Foundation of Jiangsu Province under Grant BK20210709, and in part by the Suzhou Municipal Science and Technology Bureau under Grant SYG202138. (Corresponding authors: Hongfeng Tao and Vladimir Stojanovic.)

Z. Zhuang and H. Tao are both with the Key Laboratory of Advanced Process Control for Light Industry (Ministry of Education), Jiangnan University, 1800 Lihu Road, Wuxi 214122, China (e-mails: 6191905054@stu.jiangnan.edu.cn; taohongfeng@jiangnan.edu.cn).

Y. Chen is with the School of Mechanical and Electrical Engineering, Soochow University, 8 Jixue Road, Suzhou, 215137, China (e-mail: yychen90@suda.edu.cn).

V. Stojanovic is with the Faculty of Mechanical and Civil Engineering, Department of Automatic Control, Robotics and Fluid Technique, University of Kragujevac, 36000 Kraljevo, Serbia (e-mail: vladostojanovic@mts.rs).

W. Paszke is with the Institute of Automation, Electronic and Electrical Engineering, University of Zielona Góra, Zielona Góra, Poland (e-mail: w.paszke@ice.uz.zgora.pl).

enhancing the learning efficiency and the optimality cannot be guaranteed for a specific objective. Therefore, optimal ILC methods, such as norm optimal ILC in [22], [23] and successive projection design in [24], [25], can be utilized.

As an indispensable part of the industrial processes, input constraints usually should be fully taken into consideration [26], especially when adopting optimal ILC methods. In [27], a boundary ILC for a flexible riser system with input saturation was constructed, where the issue of input saturation was handled by proposing an auxiliary term. Some research on optimal ILC design with input constraints has been also investigated, where the ILC problem is usually reformulated to a constrained optimization problem. A norm optimal ILC for time-varying linear systems with inequality constraints was revisited and generalized under deterministic, stochastic disturbances and noises in [28]. A successive projection framework for constrained ILC problems was proposed in [29], where the monotonic convergence property of the optimal ILC algorithms was derived. Moreover, the data-driven constrained optimal ILC methods for both linear and nonlinear systems were proposed in [30] and [31] respectively. Nevertheless, these constrained optimal ILC methods only discuss the feasibility and do not attempt to further improve the performance under input constraints.

Plenty of efficient optimization methods from numerical optimization theory were considered to better handle optimal ILC problems with input constraints. In [32], the barrier method was introduced in the ILC algorithm design, where the restriction that global optimal solution of the unconstrained problem should exist in the constraint set was removed. In addition, the ILC design with barrier method was extended to the point-to-point tracking task in [33]. In contrast to the barrier method, the primal-dual interior point method was considered in [34], while it focuses more on the reduction of computational complexity during the optimal ILC process by use of the sequentially semi-separable structure. In [35], a Newton-type optimization method was introduced in the data-driven ILC design and the monotonic convergence of tracking errors was thus theoretically guaranteed under specific circumstances. However, the convergence criterion was seldom given for certain optimal performance in aforementioned optimization method ILC designs, except for [36], where the criteria for monotonic and global convergence were presented for general first-order ILC laws with projection.

Since the interior point designs above are all based on the 2-norm cost function, a modified interior point method was used in optimal ILC design with non-smooth type cost functions in [37]. In [38], the BFGS (Broyden, Fletcher, Goldfarb, Shanno) optimization algorithm was extended to ILC design under input inequality constraints to achieve monotonic and super-linear convergence properties. Also, a new optimal ILC method under time-varying uncertainty was proposed in [39], where the ILC problem was reformulated in the framework of convex-concave game and thus it can be solved by a subgradient method. In [40], point-to-point ILC problem under bounded trial-varying initial conditions was reformulated as a worst-case norm optimal problem, which can accordingly be solved by the Lagrange dual approach. However, there

exist more complex practical implementations in most of the aforementioned methods and little convergence analysis studies are conducted in a theoretical way. Besides, uncertainties against ILC design postulates, e.g. the nonuniform trial length problem, are seldom considered in these optimization ILC processes.

In this paper, an optimal ILC algorithm for linear time-invariant multiple-input multiple-output (MIMO) systems with nonuniform trial lengths under input constraints is developed. With modifications for the nonuniform trial length problem, the ILC problem is transformed into a constrained optimization problem and hence the primal-dual interior point method can be used to enhance the constraint handling capability during the ILC process. Moreover, monotonic convergence property of the modified tracking error is achieved in the sense of mathematical expectation. Robustness of the proposed algorithm to both model uncertainty and nonuniform trial lengths are analyzed. A mobile robot with two independent driving wheels is chosen as a numerical simulation example to verify the effectiveness.

The main contributions are summarized as follows:

- 1) An optimal ILC algorithm for problems with nonuniform trial lengths under input constraints is developed.
- 2) Compared with the ILC approaches for nonuniform trial lengths such as in [13]–[19], the proposed algorithm enhances the input constraint handling capability by introducing the primal-dual interior point method.
- 3) Compared with the barrier method based ILC design such as in [32], [33], [37], the proposed algorithm is easier to implement and can deal with the practical situation that the input signals are not feasible.
- 4) The monotonic convergence property of the proposed algorithm is obtained in the sense of mathematical expectation.

This paper is organized as follows. First of all, the problem formulation is addressed in Section II. Section III introduces an ILC algorithm based on a primal-dual interior point method for problems with nonuniform trial lengths under input constraints. Main results of this paper are given in Section IV. Simulation verification is shown in Section V. The conclusions and future work are given in Section VI.

The main notations in this paper are listed: $E\{\cdot\}$ and $P\{\cdot\}$ denote the mathematical expectation and the probability of an event, respectively. \mathbb{N} denotes the set of natural numbers and \mathbb{R}^n and $\mathbb{R}^{n \times m}$ denote the sets of n -dimensional real vectors and $n \times m$ real matrices, respectively. T in the superscript denotes the transposed component of a vector. The superscript (i) denotes the i -th component in a vector. The inequality notation \geq and \leq for vectors means comparison on each components. $\|\cdot\|_2$ is denoted as $\|\cdot\|$ for simplicity. \otimes denotes the Kronecker product. Other notations will be introduced as required.

II. PROBLEM FORMULATION

In this section, the system dynamics is firstly introduced with mathematical notations. Then, the nonuniform trial length and input constraint problem are formulated under the lifted

system framework. The ILC design problem with nonuniform trial lengths under input constraints is finally defined.

A. System Dynamics

Consider the stable closed loop dynamics of the feedback control system with the state space form

$$\begin{cases} x_k(t+1) = Ax_k(t) + Bu_k(t), \\ y_k(t) = Cx_k(t), \end{cases} \quad (1)$$

where $t \in \mathbb{N}$ and the subscript $k \in \mathbb{N}$ denote the trial number and time index, respectively. N_d is the desired trial length with $t \in [0, N_d]$. $x_k(t) \in \mathbb{R}^n$, $u_k(t) \in \mathbb{R}^l$ and $y_k(t) \in \mathbb{R}^m$ denote the state, input and output vectors, respectively. A , B and C are system matrices with appropriate dimensions with $CB \neq 0$ for controllability of the system. $y_d(t)$ is defined as the desired output trajectory. The initial condition satisfies $E\{x_k(0)\} = x_d(0)$.

Reformulating the system (1) into a lifted system framework along the trial yields

$$y_k = Gu_k + d_k, \quad (2)$$

where

$$u_k = [u_k^T(0), u_k^T(1), \dots, u_k^T(N_d - 1)]^T, \quad (3)$$

$$y_k = [y_k^T(1), y_k^T(2), \dots, y_k^T(N_d)]^T. \quad (4)$$

G and d_k denote the system model and the effect of the initial conditions respectively, i.e.

$$G = \begin{bmatrix} CB & 0 & 0 & \dots & 0 \\ CAB & CB & 0 & \dots & 0 \\ CA^2B & CAB & CB & \dots & 0 \\ \vdots & \vdots & \vdots & \ddots & \vdots \\ CA^{N_d-1}B & CA^{N_d-2}B & CA^{N_d-3}B & \dots & CB \end{bmatrix}, \quad (5)$$

$$d_k = \begin{bmatrix} (CA)^T & (CA^2)^T & \dots & (CA^{N_d})^T \end{bmatrix}^T x_k(0). \quad (6)$$

By $E\{x_k(0)\} = x_d(0)$, d_d is given as

$$d_d = \begin{bmatrix} (CA)^T & (CA^2)^T & \dots & (CA^{N_d})^T \end{bmatrix}^T x_d(0), \quad (7)$$

and the desired output vector y_d is

$$y_d = [y_d^T(1), y_d^T(2), \dots, y_d^T(N_d)]^T. \quad (8)$$

B. Modified ILC Problem Definition

Classical ILC schemes requires that every trial operates with a fixed duration. For the nonuniform trial length situation, the available error information can still be useful for the subsequent trial. To better utilize such available information for optimal ILC design, zero signal values can be appended to the absent time instances. Moreover, set the desired trial length as the maximum one, then the modified tracking error is defined as

$$e_k = \begin{bmatrix} \underbrace{e_k^T(1), \dots, e_k^T(N_k)}_{N_k}, 0, \dots, 0 \end{bmatrix}^T, \quad (9)$$

where N_k denotes the actual trial length of the k -th trial. Denote the minimum actual length by N_m , then N_k randomly varies within $\{N_m, N_m + 1, \dots, N_d\}$. Hence there will be $n_s = N_d - N_m + 1$ possible trial lengths in total. Define the probability of $N_m, N_m + 1, \dots, N_d$ appearing along the trial as p_1, p_2, \dots, p_{n_s} respectively, then

$$\sum_{i=1}^{n_s} p_i = 1, \quad (10)$$

where $p_i > 0$, for $1 \leq i \leq n_s$. A random matrix is introduced as

$$M_k = \begin{bmatrix} I_{N_k} \otimes I_m & \mathbf{0} \\ \mathbf{0} & \mathbf{0} \end{bmatrix} \in \mathbb{R}^{(m \cdot N_d) \times (m \cdot N_d)}, \quad (11)$$

where I_l denotes unit matrix with dimension of $l \times l$ and $\mathbf{0}$ denotes the zero matrix with appropriate dimension. Then

$$e_k = M_k (y_d - y_k). \quad (12)$$

To calculate the mathematical expectation of the random matrix, another random variables $\chi_k(t) \in \{0, 1\}$ is introduced to represent whether the output occurs at time t at the k -th trial as in [16]. For simplicity, the mathematical expectation of different dimensions in random matrix is set identical. Let $\chi_k(t) = 1$ represents the event that the output of time t occurs. Denote its probability by $p(t)$, then

$$p(t) = P\{\chi_k(t) = 1\} = \begin{cases} 1, & t \leq N_m - 1, \\ \sum_{i=t-N_m+1}^{n_s} p_i, & N_m \leq t \leq N_d, \end{cases} \quad (13)$$

which yields $E\{\chi_k(t)\} = p(t)$, hence

$$\begin{aligned} E\{M_k\} &= \text{diag} \left\{ \underbrace{1, 1, \dots, 1}_{N_m-1}, E\{\chi_k(N_m)\}, \dots, E\{\chi_k(N_d)\} \right\} \otimes I_m \\ &= \text{diag} \left\{ \underbrace{1, 1, \dots, 1}_{N_m-1}, p(N_m), \dots, p(N_d) \right\} \otimes I_m \triangleq \bar{M}. \end{aligned} \quad (14)$$

C. Input Constraints

Taking the safety reason or the limitations of actuators into considerations, input constraints always exist in practice and are often expressed in the form of mathematical inequalities. Three practical forms of input constraints are listed.

- Input saturation constraint:

$$u_{\min} \leq u_{k+1} \leq u_{\max}, \quad (15)$$

where u_{\min} and u_{\max} are the lower and upper bounds of the input vector u_{k+1} .

- Input increment constraint with respect to the trial index:

$$\Delta u_{\min} \leq \Delta u_{k+1} = u_{k+1} - u_k \leq \Delta u_{\max}, \quad (16)$$

where Δu_{\min} and Δu_{\max} are the lower and upper bounds on the change of control input along the trial index.

- Input increment constraint with respect to the time index:

$$\delta u_{\min} \leq \delta u_{k+1}(t) = u_{k+1}(t) - u_{k+1}(t-1) \leq \delta u_{\max}, \quad (17)$$

where δu_{\min} and δu_{\max} are the lower and upper bounds on the change of control input along the time index.

Moreover, the constraint (16) is changed to be

$$\Delta u_{\min} + u_k \leq u_{k+1} \leq \Delta u_{\max} + u_k. \quad (18)$$

Assume $\delta u_k(0) = u_k(0)$, then

$$\delta u_{k+1} = \mu u_{k+1}, \quad (19)$$

where

$$\mu = \begin{bmatrix} I_l & 0_l & \cdots & 0_l & 0_l \\ -I_l & I_l & \cdots & 0_l & 0_l \\ 0_l & -I_l & \ddots & \vdots & 0_l \\ \vdots & \ddots & \ddots & \ddots & \vdots \\ 0_l & 0_l & \cdots & -I_l & I_l \end{bmatrix} \in \mathbb{R}^{(l \cdot N_d) \times (l \cdot N_d)}. \quad (20)$$

Then, reformulate (17) as

$$\delta u_{\min} \leq \mu u_{k+1} \leq \delta u_{\max}, \quad (21)$$

Finally, the three input constraints are organized as

$$\zeta_u u_{k+1} \geq \zeta_{k+1}, \quad (22)$$

where

$$\zeta_u = \begin{bmatrix} I \\ -I \\ \mu \\ -\mu \end{bmatrix}, \zeta_{k+1} = \begin{bmatrix} \max(u_{\min}, \Delta u_{\min} + u_k) \\ -\min(u_{\max}, \Delta u_{\max} + u_k) \\ \delta u_{\min} \\ -\delta u_{\max} \end{bmatrix}, \quad (23)$$

where I is the identity matrix with appropriate dimension. Note that the inequality constraints on u_{k+1} defined in (22) is associated with u_k , which means the scope of input constraints may vary along the trial. This is because the input saturation constraint and the input increment constraint with respect to the trial index influence each other to some extent. Nonetheless, the global input constraint set, denoted by Ω , is still a convex set according to the definition of (15), (16) and (17).

D. ILC Design Problem

The ILC design problem in this paper is given as follows:

Definition 1: The ILC design problem with nonuniform trial lengths under input constraints aims at designing an input update law

$$u_{k+1} = f(u_k, u_{k-1}, \dots, e_k, e_{k-1}, \dots), \quad (24)$$

which consists of historical input and tracking error information, such that the modified tracking error converges to zero as $k \rightarrow \infty$ in the sense of mathematical expectation along the trials, namely,

$$\lim_{k \rightarrow \infty} \|E\{e_k\}\| = 0. \quad (25)$$

Definition 1 describes the problem discussed in this paper with simple and clear mathematical expression, which provides the necessary theoretical basis for the control algorithm design next.

III. CONSTRAINED ILC DESIGN

In this section, the constrained ILC problem is reformulated as a quadratic programming (QP) problem, so some efficient numerical optimization methods with iterative search schemes, e.g. interior point methods, can be employed to solve it. By embedding experimental data in each iteration, an ILC algorithm can be developed to solve the ILC design problem in Definition 1.

A. Reformulated as a QP Problem

A cost function is firstly defined for the ILC design problem in Definition 1, which consists of the weighting norms of both modified error and control input increment. As an additional term, the input increment is a necessary condition for optimal ILC algorithms to achieve complete tracking and results in the smoothness of input signals. The cost function is defined as

$$J(u_{k+1}) = \|E\{e_{k+1}\}\|_Q^2 + \|u_{k+1} - u_k\|_R^2, \quad (26)$$

where Q and R are symmetric positive definite weighing matrices with appropriate dimensions. Then, substituting (12) into the cost function (26) and transforming it into the form with respect to u_{k+1} yield

$$J(u_{k+1}) = u_{k+1}^T (G^T \bar{K} G + R) u_{k+1} - 2 [u_k^T (G^T \bar{K} G + R) + e_k^T Q \bar{M} G] u_{k+1} + d, \quad (27)$$

where $\bar{K} = \bar{M}^T Q \bar{M}$ and

$$d = u_k^T R u_k + (y_d - d_d)^T \bar{K} (y_d - d_d).$$

Therefore, the constrained ILC problem can be reformulated as a QP problem under inequality constraints, i.e.,

$$\begin{aligned} \min_{u_{k+1}} \quad & J(u_{k+1}) = \frac{1}{2} u_{k+1}^T H u_{k+1} + c^T u_{k+1} + d \\ \text{s.t.} \quad & \zeta_u u_{k+1} - \zeta_{k+1} \geq 0, \end{aligned} \quad (28)$$

where

$$\begin{aligned} H &= 2 (G^T \bar{K} G + R), \\ c^T &= -2 [u_k^T (G^T \bar{K} G + R) + e_k^T Q \bar{M} G], \end{aligned}$$

and H is a positive definite matrix since the weighting matrices Q and R are positive definite.

B. Primal-Dual Interior Point Method Design

The primal-dual interior point method is employed to solve the inequality constrained QP problem, which can hence develop an ILC algorithm for the ILC design problem defined by Definition 1. To begin with, an efficient primal-dual interior point method is introduced. Define the dual variable $\lambda \in \mathbb{R}^s$ with $s = 4l \cdot N_d$. Since H is positive definite, the optimal solution of (28) is unique and satisfies the following Karush-Kuhn-Tucker (KKT) conditions:

$$\begin{aligned} H u_{k+1} + c - \zeta_u^T \lambda &= 0, \\ \zeta_u u_{k+1} - \zeta_{k+1} &\geq 0, \\ (\zeta_u u_{k+1} - \zeta_{k+1})^{(i)} \lambda^{(i)} &= 0, \quad i = 1, 2, \dots, s, \\ \lambda &\geq 0. \end{aligned} \quad (29)$$

Introduce the slack variable $\omega \in \mathbb{R}^s$ to give rise to the modified KKT conditions:

$$\begin{aligned} Hu_{k+1} + c - \zeta_u^T \lambda &= 0, \\ \zeta_u u_{k+1} - \zeta_{k+1} - \omega &= 0, \\ \Lambda W \beta &= \varphi \beta, \\ \lambda, \omega &\geq 0, \end{aligned} \quad (30)$$

where

$$\begin{aligned} \Lambda &= \text{diag} \left(\lambda^{(1)}, \lambda^{(2)}, \dots, \lambda^{(s)} \right), \\ W &= \text{diag} \left(\omega^{(1)}, \omega^{(2)}, \dots, \omega^{(s)} \right), \\ \beta &= [1, 1, \dots, 1]^T \in \mathbb{R}^s, \\ \varphi &= \delta \cdot \theta / s, \quad \delta \in (0, 1). \end{aligned}$$

$\theta = \lambda^T \omega$ denotes the complementarity in the path-following methods, which can be also seen as the duality gap for the convex problem (28). Decreasing θ yields that the solution of the modified KKT conditions (30) converges to the global optimal solution. For arbitrary $\varphi > 0$, the solution of modified KKT conditions (30) is unique and denote it as $u_{k+1}(\varphi), \lambda(\varphi), \omega(\varphi)$. In addition, $\{u_{k+1}(\varphi), \lambda(\varphi), \omega(\varphi) | \varphi > 0\}$ is defined as the central path of the primal problem (28). By reducing φ continuously, duality gap gets smaller so as to keep approaching to the global optimal solution.

When fixing φ and applying Newton's method, substitute $(u_{k+1}, \lambda, \omega)$ in (30) with $(u_k + \Delta \bar{u}_{k+1}, \lambda + \Delta \lambda, \omega + \Delta \omega)$ and ignore the quadratic terms, then we have

$$\begin{bmatrix} -H & \zeta_u^T & 0 \\ \zeta_u & 0 & -I_s \\ 0 & W & \Lambda \end{bmatrix} \begin{bmatrix} \Delta \bar{u}_{k+1} \\ \Delta \lambda \\ \Delta \omega \end{bmatrix} = \begin{bmatrix} \sigma \\ \rho \\ \varphi \beta - \Lambda W \beta \end{bmatrix}, \quad (31)$$

where

$$\begin{aligned} \sigma &= Hu_k + c - \zeta_u^T \lambda, \\ \rho &= \zeta_{k+1} - \zeta_u u_k + \omega, \end{aligned}$$

and $\Delta \bar{u}_{k+1}, \Delta \lambda$ and $\Delta \omega$ denote the step directions.

The step directions will be obtained by computing (31) subject to the condition that the step length α is 1. Nonetheless, it is only required both dual and slack variables are positive definite as in (30), i.e.,

$$\begin{aligned} \lambda^{(i)} + \alpha^{\text{pri}} \Delta \lambda^{(i)} &> 0, \\ \omega^{(j)} + \alpha^{\text{dual}} \Delta \omega^{(j)} &> 0, \end{aligned} \quad i, j = 1, 2, \dots, s, \quad (32)$$

where α^{pri} and α^{dual} denote the step lengths demanding the positive definite of the dual and slack variables respectively. Introduce a parameter $\tau \in (0, 1)$ to achieve the equality, then

$$\alpha^{\text{pri}} = \max \left\{ \alpha : \tau \lambda^{(i)} + \alpha \Delta \lambda^{(i)} \geq 0, i = 1, 2, \dots, s \right\}, \quad (33)$$

$$\alpha^{\text{dual}} = \max \left\{ \alpha : \tau \omega^{(j)} + \alpha \Delta \omega^{(j)} \geq 0, j = 1, 2, \dots, s \right\}, \quad (34)$$

where τ is often close to but strictly less than 1 so as to accelerate the convergence.

Note that σ, ρ and θ correspond to left-hand side of the first three equations defined in the modified KKT conditions

(30). Therefore, by introducing a stopping parameter ϵ , we can claim that an approximately optimal solution of (28) is obtained if $\|\sigma\| < \epsilon, \|\rho\| < \epsilon$ and $\|\varphi\| < \epsilon$. Although the primal-dual interior point method is really Newton's method supplemented by variable step lengths, the cost function is improved at each trial. An extensive study about the primal-dual interior point method can be referred to [41]. Moreover, it is better to choose an initial point that is far away from the boundary where $\lambda, \omega = 0$. In this case, the optimization process may take long steps in the first few trials. Further choice of the initial point can be referred to [42].

C. A Constrained Optimal ILC Algorithm

By calculating the step directions and lengths as (31), (33) and (34), a practical optimal ILC algorithm for the nonuniform trial length problem under input constraints can be developed. The main modification of the proposed optimal ILC algorithm compared to the primal-dual interior point method lies in the use of experimental data, and hence one trial corresponds to one update of step directions of Newton's method in (31).

Algorithm 1 A Constrained Optimal ILC Algorithm

Input: System dynamics (1), weighting matrices Q, R , initial input $u_0 \in \Omega$ and $\lambda_0, \omega_0 > 0$, parameters $\delta \in (0, 1)$, $\tau \in (0, 1)$ and $\epsilon > 0$.

Output: A sequence $\{u_k\}_{k \geq 0}$ to solve the ILC design problem in Definition 1.

- 1: **repeat**
- 2: Calculate the two step lengths α_k^{pri} and α_k^{dual} using (33) and (34);
- 3: Set the step length $\alpha_k = \min \left\{ \alpha_k^{\text{pri}}, \alpha_k^{\text{dual}} \right\}$ with $\alpha_k \in (0, 1]$;
- 4: Calculate σ, ρ and φ in (31);
- 5: Solve (31) to get the step directions $\Delta \bar{u}_{k+1}, \Delta \lambda_{k+1}$ and $\Delta \omega_{k+1}$;
- 6: Set

$$u_{k+1} \leftarrow u_k + \alpha_k \Delta \bar{u}_{k+1}, \quad (35)$$

$$\lambda_{k+1} \leftarrow \lambda_k + \alpha_k \Delta \lambda_{k+1}, \quad (36)$$

$$\omega_{k+1} \leftarrow \omega_k + \alpha_k \Delta \omega_{k+1}; \quad (37)$$

7: **until** $\|\sigma\| < \epsilon, \|\rho\| < \epsilon$ and $\|\varphi\| < \epsilon$

8: **return** $\{u_k\}_{k \geq 0}$.

The general block diagram of the proposed ILC design is given in the left-hand side of Fig. 1. Different from the ILC design using the barrier method such as in [32], [33], [37], there is only one layer of loop in the primal-dual method design, where associated auxiliary variables are simultaneously updated for an easier implementation. The general block diagram of the barrier method design is also given in the right-hand side of Fig. 1. Note that there are both inner and outside loop in the barrier method ILC design typically, where the input signals should be strictly feasible.

Remark 1: When it comes to the optimal control of complex nonlinearities and unknown dynamics, the intelligent critic framework for advanced optimal control, as investigated in

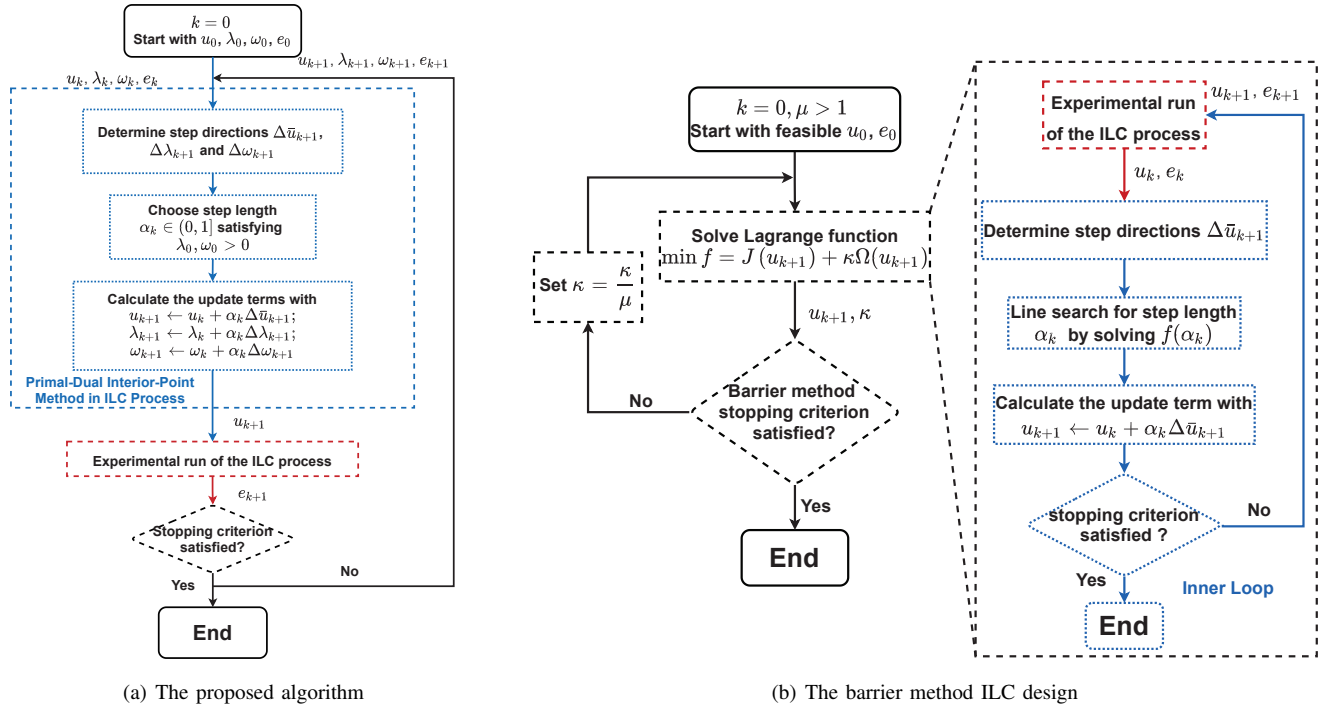


Fig. 1. The general block diagrams of two interior point methods in ILC design.

[43], [44], can be considered as a potential direction, where reinforcement learning is regarded as a key learning mechanism. Fortunately, there have been some studies on the combinations of reinforcement learning and ILC as in [45], [46].

To explain how Algorithm 1 can solve the ILC design problem in Definition 1, a proposition is presented as follows.

Proposition 1: The input sequence generated by Algorithm 1 iteratively solves the ILC design problem in Definition 1.

Proof: Given initial control input signals u_0 , as well as modified problem definition for nonuniform trial lengths, the control input sequence generated by (35) in Algorithm 1 is within input constraints.

Furthermore, the input signals of next trial always continue to the time instant N_d no matter when the next trial stops. Therefore, Algorithm 1 is causal in practice and hence can solve the ILC design problem in Definition 1 iteratively. ■

A causal ILC algorithm for the nonuniform trial length problem is proposed by using the primal-dual interior method to deal with the input constraints. In next section, the convergence properties of the designed ILC system will be discussed.

IV. MAIN RESULTS

Before conducting the convergence analysis, a typical assumption on the input signal is given firstly.

Assumption 1: There exists a desired input $u_d \in \Omega$ such that the tracking error of systems with nonuniform trial lengths converges to zero in the sense of mathematical expectation.

Assumption 1 ensures that systems with nonuniform trial lengths are possible to achieve the zero tracking error for certain reference trajectory in the sense of mathematical expectation.

A. Boundedness of Input Signal

To begin with, a technical lemma is introduced to ensure that the solution of (29) is the global solution of (28).

Lemma 1: If u_∞ satisfies the conditions (29) for $\lambda^{(i)}$, $i = 1, 2, \dots, s$, and H is positive definition, then u_∞ is a global solution of (28).

Proof: See Theorem 16.4 in [47] for more details. ■

With Lemma 1, the result that Algorithm 1 can find out the global solution of (28) is given next.

Theorem 1: When Assumption 1 holds, given systems described by (1), apply Algorithm 1 yields that the input sequence $\{u_k\}_{k \geq 0}$ converges to the global solution u_∞ of the constrained QP problem (28).

Proof: Firstly, add trial index to ρ , σ and θ in (31). Substituting update law (35) and (37) of Algorithm 1 into ρ_{k+1} yields

$$\rho_{k+1} = \rho_k - \alpha_k (\zeta_u \Delta \bar{u}_{k+1} - \Delta \omega_{k+1}). \quad (38)$$

It follows from (31) that

$$\zeta_u \Delta \bar{u}_{k+1} - \Delta \omega_{k+1} = \rho_k, \quad (39)$$

then

$$\rho_{k+1} = (1 - \alpha_k) \rho_k, \quad (40)$$

and similarly

$$\sigma_{k+1} = (1 - \alpha_k) \sigma_k. \quad (41)$$

For the duality gap, there exists

$$\begin{aligned} \theta_{k+1} &= \lambda_{k+1}^T \omega_{k+1} \\ &= (\lambda_k + \alpha_k \Delta \lambda_{k+1})^T (\omega_k + \alpha_k \Delta \omega_{k+1}) \\ &= \theta_k + \alpha_k (\Delta \lambda_{k+1}^T \omega_k + \lambda_k^T \Delta \omega_{k+1}) \\ &\quad + \alpha_k^2 \Delta \lambda_{k+1}^T \Delta \omega_{k+1}, \end{aligned} \quad (42)$$

where

$$\begin{aligned}\Delta\lambda_{k+1}^T\omega_k + \lambda_k^T\Delta\omega_{k+1} &= \beta^T(W_k\Delta\lambda_{k+1} + \Lambda_k\Delta\omega_{k+1}) \\ &= \beta^T(\varphi_k\beta - \Lambda_k W_k\beta) \\ &= \delta\theta_k - \theta_k.\end{aligned}\quad (43)$$

Then, substituting (43) to (42) and ignoring the quadratic terms $\Delta\lambda_{k+1}^T\Delta\omega_{k+1}$ yield

$$\theta_{k+1} = [1 - (1 - \delta)\alpha_k]\theta_k. \quad (44)$$

Moreover, since $\alpha_k \in (0, 1]$, it follows from (40) that

$$\|\rho_{k+1}\| \leq (1 - \alpha_k)\|\rho_k\| \leq \dots \leq (1 - \alpha_k)^{k+1}\|\rho_0\|, \quad (45)$$

and similarly

$$\|\sigma_{k+1}\| \leq (1 - \alpha_k)\|\sigma_k\| \leq \dots \leq (1 - \alpha_k)^{k+1}\|\sigma_0\|. \quad (46)$$

For (44), it follows that

$$\theta_{k+1} \leq [1 - (1 - \delta)\alpha_k]\theta_k \leq \dots \leq [1 - (1 - \delta)\alpha_k]^{k+1}\theta_0. \quad (47)$$

Combining (45), (46) and (47) with $\delta \in (0, 1)$ and $\alpha_k \in (0, 1]$, a solution that satisfies the KKT condition (29), i.e. u_∞ , is eventually found as $k \rightarrow \infty$, namely,

$$\lim_{k \rightarrow \infty} u_k = u_\infty. \quad (48)$$

Therefore, since H is positive definite, u_∞ is the global solution of the constrained optimization problem (28) according to Lemma 1 and the proof is complete. ■

After finding the global solution u_∞ , the relationship between u_∞ and u_d in Assumption 1 is explored to show the convergence properties of Algorithm 1.

B. Convergence Properties of Algorithm 1

Given the need for convergence analysis, the cost function can be seen as a point with respect to both the tracking error and input signal, i.e., $J(u_{k+1})$ can be denoted by $J(E\{e_{k+1}\}, u_{k+1})$ as required. Then, a theorem for convergence properties of Algorithm 1 is given.

Theorem 2: When Assumption 1 holds, given systems described by (1), applying Algorithm 1 yields

$$\|E\{e_k\}\| \geq \|E\{e_{k+1}\}\|, \quad (49)$$

and

$$\lim_{k \rightarrow \infty} \|E\{e_{k+1}\}\| = 0. \quad (50)$$

Proof: For the cost function (26), applying Algorithm 1 yields

$$\begin{aligned}J(E\{e_k\}, u_k) &= \|E\{e_k\}\|_Q^2 \\ &\geq J(E\{e_{k+1}\}, u_{k+1}) \\ &= \|E\{e_{k+1}\}\|_Q^2 + \|u_{k+1} - u_k\|_R^2,\end{aligned}\quad (51)$$

then the monotonic convergence property (49) is obtained.

Moreover, substitute the update law of u_{k+1} (35) to the tracking error (12) and fix $\Delta\bar{u}_{k+1} = 0$, then

$$E\{e_{k+1}\} = E\{e_k\} - \bar{M}G\alpha_k\Delta\bar{u}_{k+1} = E\{e_k\}, \quad (52)$$

which means $(E\{e_k\}, u_{k+1})$ is also a feasible point in the convex set Ω . Then, it follows from (51) that

$$\begin{aligned}J(E\{e_k\}, u_k) - \Delta u_{k+1}^T R \Delta u_{k+1} \\ = J(E\{e_k\}, u_{k+1}) \\ \geq J(E\{e_{k+1}\}, u_{k+1}) \geq 0,\end{aligned}\quad (53)$$

which yields

$$J(E\{e_0\}, u_0) \geq J(E\{e_{k+1}\}, u_{k+1}) + \sum_{i=1}^{k+1} \Delta u_i^T R \Delta u_i \geq 0. \quad (54)$$

Since $J(E\{e_0\}, u_0) < \infty$, then

$$\lim_{k \rightarrow \infty} \Delta u_{k+1} = 0. \quad (55)$$

Recall that $(E\{e_\infty\}, u_\infty)$ is the global solution of the constrained optimization problem (28), so any direction of the directional derivative with respect to the cost function (26) at the point $(E\{e_\infty\}, u_\infty)$ is no less than zero. Considering the directional derivative from $(E\{e_\infty\}, u_\infty)$ to $(0, u_d)$ defined in Assumption 1, it follows that

$$\begin{aligned}\nabla J^T|_{(E\{e_\infty\}, u_\infty)} \cdot \begin{bmatrix} -E\{e_\infty\} \\ u_d - u_\infty \end{bmatrix} \\ = [E\{e_\infty^T\} Q \quad \Delta u_\infty^T R] \cdot \begin{bmatrix} -E\{e_\infty\} \\ u_d - u_\infty \end{bmatrix} \\ = -E\{e_\infty^T\} Q E\{e_\infty\} + \Delta u_{k+1}^T R (u_d - u_\infty) \geq 0,\end{aligned}\quad (56)$$

which yields

$$\Delta u_\infty^T R u_d \geq E\{e_\infty^T\} Q E\{e_\infty\} + \Delta u_{k+1}^T R u_\infty \geq 0, \quad (57)$$

and hence $\lim_{k \rightarrow \infty} \|E\{e_{k+1}\}\| = 0$ according to (55). Finally, (50) is obtained and the proof is complete. ■

Theorem 2 reveals that applying Algorithm 1 yields the tracking error converges to zero in the sense of mathematical expectation with $u_\infty = u_d$. In other words, the sequence $\{u_k\}_{k \geq 0}$ generated by Algorithm 1 can converge to the desired input in Assumption 1. Nonetheless, Assumption 1 is not always true in practice, and hence it is also important to investigate the case that Assumption 1 does not hold. For the convex QP problem under inequality constraints, the global solution must be on the boundary of convex constraint set. When Assumption 1 does not hold, denote the optimal solution under inequality constraints as u_s^* , then each component of u_s^* may reach to the boundary or partially, which depends on the relationship between Ω and u_d . Moreover, a corollary is given as follows.

Corollary 1: When Assumption 1 does not hold, given systems with nonuniform trial lengths (1), applying Algorithm 1 yields

$$\lim_{k \rightarrow \infty} \|E\{e_k\}\| = \|\bar{M}(y_d - G u_s^* - d_d)\|. \quad (58)$$

Proof: Under input constraints, the input signal cannot converge to u_d , which yields

$$\lim_{k \rightarrow \infty} u_k = u_s^*. \quad (59)$$

Then, according to the result of Theorem 2, (58) is obtained and the proof is complete. ■

In Corollary 1, the convergence boundary is obtained when Assumption 1 does not hold. Furthermore, Algorithm 1 can take a nontrivial step along each trial to get closer to the theoretical boundary derived from Corollary 1.

C. Robustness Analysis

From the practical point of view, the control input under nominal model is not enough to show the efficacy of the proposed algorithm. Therefore, the robustness of Algorithm 1 against model uncertainty is investigated, where a bounded additional modeling error factor Δ_G that varies along the time is employed. The uncertainty model is defined as

$$\hat{G} = G(I + \Delta_G). \quad (60)$$

Definition 2: The ILC update law (35) is referred to as *robust monotonic convergent (RMC)* if there exists α_k for each $k \in \mathbb{N}$ such that $J(u_k + \alpha_k \Delta \hat{u}_{k+1}) \leq J(u_k)$ with respect to uncertainty model \hat{G} , where \hat{u}_{k+1} is the solution of (31) under uncertainty model. In other words, the cost function is non-increasing.

Theorem 3: Algorithm 1 is RMC if there exists γ satisfying $\|\Delta_G\| < \gamma$ such that

$$\left\| \Delta \hat{K} + R \right\| \leq \frac{2}{\|\Delta \hat{u}_{k+1}\|} \left(\left\| \hat{G} \bar{K} (y_d - d_d) \right\| + \left\| \Delta \hat{K} u_k \right\| \right), \quad (61)$$

for each $k \in \mathbb{N}$, where $\Delta \hat{K} = \hat{G}^T \bar{K} \hat{G}$.

Proof: According to Definition 2, if Algorithm 1 is RMC, the cost function is non-increasing for any bounded modeling error Δ_G , i.e.

$$\max_{\Delta_G} J(u_k + \alpha_k \Delta \hat{u}_{k+1}) \leq J(u_k). \quad (62)$$

Substituting the cost function (26) yields

$$\max_{\Delta_G} \left\{ \|E\{e_{k+1}\}\|_Q^2 + \|u_{k+1} - u_k\|_R^2 \right\} \leq \|E\{e_k\}\|_Q^2, \quad (63)$$

which can be reformulated as

$$\|\Delta \hat{u}_{k+1}\|_{(\Delta \hat{K} + R)}^2 \leq 2\Delta \hat{u}_{k+1}^T \left(\hat{G}^T \bar{K} (y_d - d_d) - \Delta \hat{K} u_k \right), \quad (64)$$

for $\alpha \in (0, 1)$. Then, (61) is obtained by utilizing the property of induced norm. ■

Remark 2: For unmodeled dynamics and uncertainties in ILC, a potential direction is to employ the new fuzzy logic systems to learn the behavior of the unknown dynamics due to the universal approximation property. To be more specific, the type-3 fuzzy logic system can be considered due to its better uncertainty modeling capability in contrast to type-1 and type-2 fuzzy systems. Since the effects of uncertainties and unmodeled dynamics are just handled by ILC itself as is shown in Theorem 3, the type-3 logic system can be embedded in the ILC design to further suppress them. More investigations of fuzzy logic systems in ILC can be referred to [48], [49] and the latest research results of fuzzy logic systems, including the type-3 fuzzy logic system, can be obtained in [50]–[53].

In addition, the variation of trial lengths is also a kind of uncertainty. To check the robustness of Algorithm 1 against the varying trial lengths, a performance index, which can be

seen as the variance of modified error vectors, is introduced as follows. To begin with, a property of the varying trial length problem is introduced, i.e.

$$P\{\chi_k(a)\chi_k(b) = 1\} = P\{\chi_k(a) = 1\} = p(a), \quad a > b, \quad (65)$$

for any $a, b \in [1, N_d]$. In other words, if there exists an output at the later time instant, there must exist an output at the previous time instant, but the opposite is not necessarily true. Then, based on the property (65), the variance of error vector can be calculated by

$$\begin{aligned} D\{e_{k+1}\} &= E\left\{ (e_{k+1} - E\{e_{k+1}\})(e_{k+1} - E\{e_{k+1}\})^T \right\} \\ &= E\{D_p\} Z - \bar{M} Z \bar{M}^T, \end{aligned} \quad (66)$$

where

$$\begin{aligned} Z &= (y_d - G u_{k+1} - d_d)(y_d - G u_{k+1} - d_d)^T, \\ E\{D_p\} &= \begin{bmatrix} p(1) & p(2) & p(3) & \cdots & p(N_d) \\ p(2) & p(2) & p(3) & \cdots & p(N_d) \\ p(3) & p(3) & p(3) & \cdots & \vdots \\ \vdots & \cdots & \cdots & \ddots & \vdots \\ p(N_d) & \cdots & \cdots & \cdots & p(N_d) \end{bmatrix} \otimes I_m. \end{aligned}$$

By the performance index (66), comparisons with other ILC designs can be conducted to verify the effectiveness of the proposed algorithm under the nonuniform trial length problem, which will be presented in the next section.

V. NUMERICAL SIMULATION VERIFICATIONS

To verify the effectiveness of the proposed algorithm, a numerical model of mobile robot with two independent driving wheels in [54] is employed. By controlling the driving voltages u_r and u_l of each wheel, both linear velocity v and azimuth ϕ of the mobile robot can be taken in control so that the mobile robot can perform trajectory tracking tasks on a fixed two-dimensional rectangular coordinate system.

A. Simulation Specification

Define the state variable of the mobile robot as $x = [v \ \phi \ \dot{\phi}]^T$, the input variable as $u = [u_r \ u_l]^T$, and the output variable as $[v \ \phi]^T$. Set the repeating operation period as $T = 2s$ and the sampling period as $0.05s$, which yields $N_d = 40$. Then, the discrete-time state-space parameters are

$$\begin{aligned} A &= \begin{bmatrix} 0.9975 & 0 & 0 \\ 0 & 1 & 0.0499 \\ 0 & 0 & 0.9955 \end{bmatrix}, \\ B &= \begin{bmatrix} 0.0125 & 0.0125 \\ -0.0021 & -0.0042 \\ -0.0833 & -0.1666 \end{bmatrix}, C = \begin{bmatrix} 1 & 0 & 0 \\ 0 & 1 & 0 \end{bmatrix}. \end{aligned} \quad (67)$$

When a mobile robot is going to move along a specific desired trajectory under control of ILC algorithms, some output constraints usually arise from the obstacles on the trajectory, which may lead to the problem with nonuniform trial lengths. Typically, the running trajectory of the robot deviates greatly from the expected one in the first few trials,

and gets closer as the progress of the ILC process. Although the obstacles are sometimes far from the desired trajectory, the output is possible to be constrained, and thus the situation that the trial length varies still happens.

In this simulation, the actual length N_k is set to satisfy the discrete uniform distribution, which means N_k varies randomly between an integer set. Let the integer set be $\{33, 34, \dots, 40\}$ and hence $p_i = 1/8$. The proposed algorithm can be used as long as the probability distribution of the actual trial length can be known. Moreover, there may exist little difference between initial azimuths of each trial due to the way of initialization in practice, while the difference may be bounded or have the same mathematical expectation. Therefore in this simulation, set initial state as a random variable with $P[x_k(0) = x^1] = P[x_k(0) = x^2] = P[x_k(0) = x^3] = 1/3$, where $x^1 = [0, 0.02, 0]^T$, $x^2 = [0, 0, 0]^T$ and $x^3 = [0, -0.02, 0]^T$. This setting satisfies $E\{x_k(0)\} = x_d(0) = [0, 0, 0]^T$. Set the initial input signal as $u_0(t) = 0, 0 \leq t \leq N_d - 1$. Also, set $k = 30$ and $N_{30} = N_d$ for better observation.

Furthermore, note that the mobile robot system (67) is a linear coupling MIMO system and can be decoupled by

$$\begin{bmatrix} u_r \\ u_l \end{bmatrix} = \begin{bmatrix} 1 & -1 \\ 0 & 1 \end{bmatrix} \begin{bmatrix} u_1 \\ u_2 \end{bmatrix}. \quad (68)$$

Then, the linear velocity v is controlled by u_1 alone and the azimuth ϕ is controlled by both u_1 and u_2 . The control procedure in this simulation is firstly to control the linear velocity v and then let the u_1 be a disturbance so that the azimuth ϕ can be controlled by u_2 alone. In this way, the robustness of the proposed algorithm against disturbances can also be verified. Set the desired trajectory of the linear velocity and the azimuth as $v_d = 1$ m/s and $\phi_d = \pi t$ rad respectively, then the desired trajectory of the mobile robot is a round.

B. Performance of the Proposed Algorithm

When applying the proposed ILC algorithm, some other parameters should be determined. Choose $\delta = 0.1$ and initial dual variable and slack variable such that $\lambda_0 = 2I_{s \times 1}$ and $\omega_0 = 2I_{s \times 1}$. Choose weighting matrices $Q = 10I_{l \cdot N_d}$ and $R = 0.001I_{l \cdot N_d}$, which also ensures the positive definite of matrix H . When Assumption 1 holds, set constraints on u_1 being $u_{\max}, u_{\min} = \pm 150V$, $\Delta u_{\max}, \Delta u_{\min} = \pm 100V$ and $\delta u_{\max}, \delta u_{\min} = \pm 100V$, and constraints on u_2 being $u_{\max}, u_{\min} = \pm 20V$, $\Delta u_{\max}, \Delta u_{\min} = \pm 20V$ and $\delta u_{\max}, \delta u_{\min} = \pm 20V$. Recall that the proposed algorithm embeds the input constraints into the ILC process actively, which means output range as well as performance can be regulated independently. Since the real input constraints on u_r and u_l can be transformed into the constraints on u_1 and u_2 by (68), so we directly set constraints on u_1 and u_2 for simplicity.

The performances of the proposed ILC algorithm are shown in Fig. 2 to Fig. 5. When Assumption 1 holds, the tracking trajectories of the 5th, 7th and 30th trials are shown in Fig. 2. The 5th and 7th trials do not run a complete trajectory because of the setting of nonuniform trial lengths. Fig. 3 respectively gives the tracking situation of both azimuth and linear velocity,

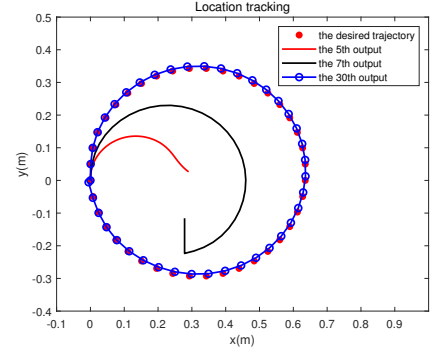


Fig. 2. Location tracking when Assumption 1 holds.

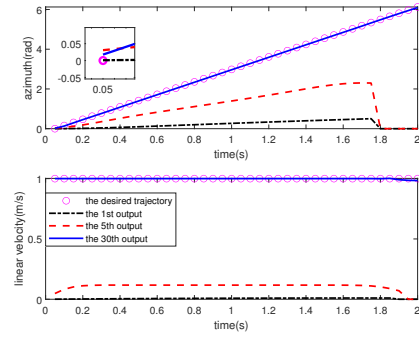


Fig. 3. Output of linear velocity and azimuth when Assumption 1 holds.

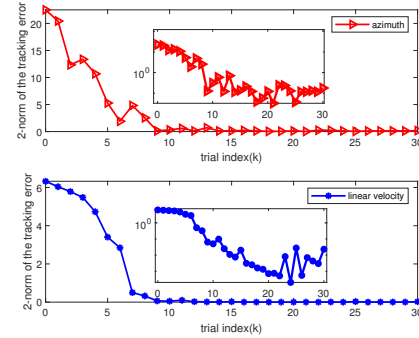


Fig. 4. Tracking error of azimuth and linear velocity when Assumption 1 holds.

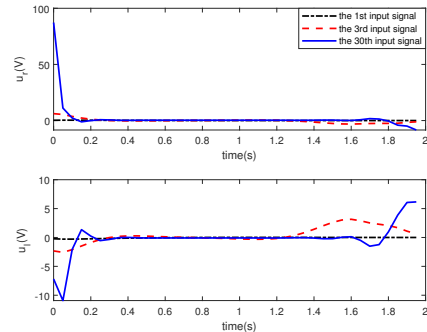


Fig. 5. Input signals of the right and left wheels when Assumption 1 holds.

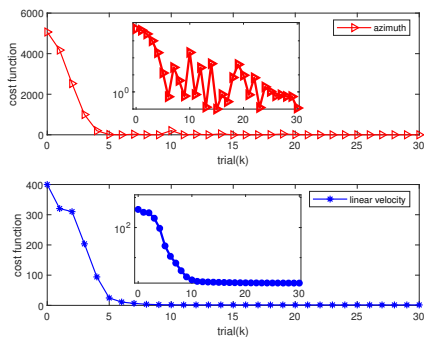


Fig. 6. Cost functions of both linear velocity and azimuth when Assumption 1 holds.

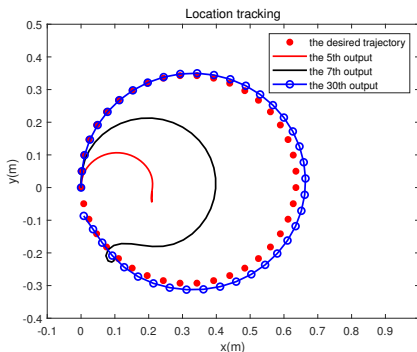


Fig. 7. Location tracking under model uncertainty on azimuth when Assumption 1 holds.

and the corresponding tracking error under both ordinary and logarithmic coordinates are shown in Fig. 4. Moreover, the 30th output cannot completely track the desired one since the varying initial state. The variation of the initial azimuths is given in Fig. 3. The input signals of the right and left wheels for the 1st, 3rd and 30th trials are shown in Fig. 5, all of which are under the input constraints. The cost functions (26) of both linear velocity and azimuth are given in Fig. 6. The cost functions converge to zero by applying the proposed algorithm, which means the ILC systems are stable. Note that the cost function of azimuth does not decrease monotonically, and this is because the initial shift is set on the azimuth.

Furthermore, the efficacy of the proposed algorithm against model uncertainty is verified. For the mobile robot, its weight or other system parameters may change when operating a specific task for many times. Therefore, the additive modeling uncertainty Δ_G is employed to further investigate the performance of the proposed algorithm. Let Δ_G vary randomly between $[-0.1, 0.1]$ and differ both in time and trial axes. When setting bounded model uncertainty on azimuth, it is shown in Fig. 7 that trajectory tracking task can be performed with a few errors after a certain number of trials.

C. Compared with Conventional Counterparts

In practice, Assumption 1 may not always hold. Therefore, it is important to verify the performance of the proposed algorithm when Assumption 1 does not hold, especially when

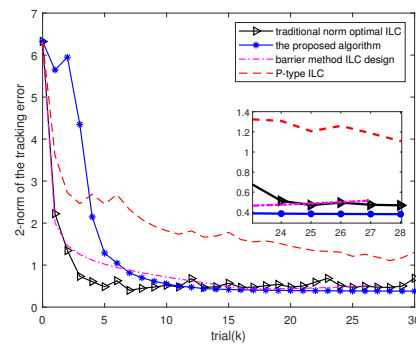


Fig. 8. Tracking error of linear velocity when Assumption 1 does not hold.

compared with other ILC designs. For simplicity, only the performance of linear velocity is presented. Set constraints on u_1 being $u_{\max}, u_{\min} = \pm 50V$, $\Delta u_{\max}, \Delta u_{\min} = \pm 10V$ and $\delta u_{\max}, \delta u_{\min} = \pm 60V$.

Choose the P-type ILC in [13], the norm optimal ILC in [40] and the barrier method ILC design in [37] as comparisons. These compared methods are all under the same nonuniform trial length and input constraint settings. The learning gain of P-type ILC is designed as Arimoto-like gain as presented in [13], whose elements on the diagonal lines are valued by 0.85. The norm optimal ILC utilizes the feedforward implementation with the same weighting matrices $Q = 10I_{l \cdot N_d}$ and $R = 0.001I_{l \cdot N_d}$. The choices of main parameters in the barrier method ILC design are as follows: the stopping criterion values of both the barrier method and its inner loop are respectively 0.0001 and 0.00001. The initial values of both κ and μ are 1 and 20, respectively.

Then, the tracking error profiles of linear velocity under the proposed algorithm as well as other three compared methods are shown in Fig. 8. Though the convergence speed is a bit slow at the first few trials, a lower convergence boundary as well as little fluctuations can be obtained by the proposed algorithm. Also, it is noted in Fig. 8 that the barrier method ILC design may stop early, and this is because the input signals of the barrier method must be strictly feasible. It is also noted that the P-type ILC is obviously slower than other three optimal ILC algorithms. Moreover, 2-norm of the variances defined in (66) are presented in Fig. 9, which demonstrates that the proposed algorithm can further suppress the effects of varying trial lengths under input constraints. Model uncertainty on linear velocity is also considered under input constraints in Fig. 10. The proposed algorithm and the barrier method ILC design have good robustness against model uncertainty, while the norm optimal ILC has a poorer performance under this circumstance.

VI. CONCLUSION AND FUTURE WORK

This paper proposed an optimal ILC algorithm for linear time-invariant MIMO systems with nonuniform trial lengths under input constraints. By reformulating the optimal ILC problem with input constraints into a QP problem, the primal-dual interior point method was employed to develop an efficient ILC algorithm for both nonuniform trial length and

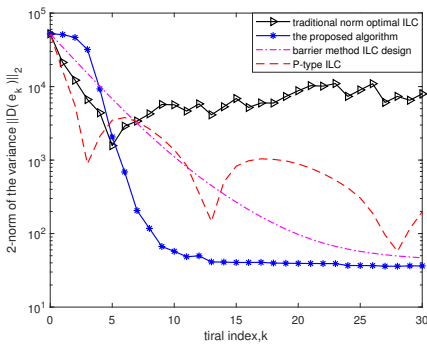


Fig. 9. 2-norm of variances with respect to tracking error of linear velocity when Assumption 1 does not hold.

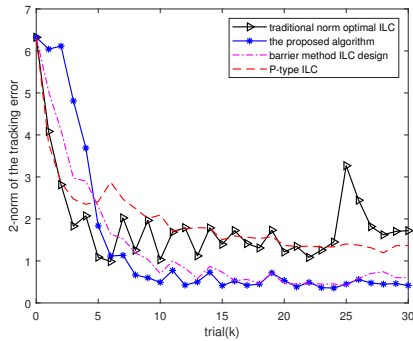


Fig. 10. Tracking error of linear velocity under model uncertainty when Assumption 1 does not hold.

input constraint problem. Compared to the similar design, i.e. the barrier method ILC design, the proposed algorithm is easier to implement and needs no strict feasible input signal. Moreover, the convergence properties of the proposed algorithm were proved theoretically, and a corollary was achieved when Assumption 1 does not hold. The effectiveness of the proposed algorithm was verified on a mobile robot model in comparison with other three conventional counterparts under same circumstances.

The future work will include experimental verification to research on the practical performance of the proposed algorithm. Also, other practical situations for the proposed algorithm, e.g. model uncertainty and non-repeatable disturbances, are going to be further investigated in the future.

REFERENCES

[1] S. Hao, T. Liu, and E. Rogers, "Extended state observer based indirect-type ILC for single-input single-output batch processes with time- and batch-varying uncertainties," *Automatica*, vol. 112, p. 108673, 2020.
 [2] H. Tao, W. Paszke, E. Rogers, H. Yang, and K. Galkowski, "Iterative learning fault-tolerant control for differential time-delay batch processes in finite frequency domains," *J. Process Control*, vol. 56, pp. 112–128, Aug. 2017.
 [3] X. Jin, "Fault-tolerant iterative learning control for mobile robots non-repetitive trajectory tracking with output constraints," *Automatica*, vol. 94, pp. 63–71, 2018.
 [4] C. T. Freeman, *Control System Design for Electrical Stimulation in Upper Limb Rehabilitation*. Cham, Switzerland: Springer, 2016.
 [5] D. Shen, G. G. Qu, and Q. J. Song, "Learning control for networked stochastic systems with random fading communication," *IEEE Trans. Syst. Man Cybern. Syst.*, vol. 52, no. 6, pp. 3659–3670, Jun. 2022.

[6] S. Arimoto, S. Kawamura, and F. Miyazaki, "Bettering operation of robots by learning," *J. Robot. Syst.*, vol. 1, no. 2, pp. 123–140, 1984.
 [7] D. A. Bristow, M. Tharayil, and A. G. Alleyne, "A survey of iterative learning control: A learning-based method for high-performance tracking control," *IEEE Control Syst. Mag.*, vol. 26, no. 3, pp. 96–114, Jun. 2006.
 [8] H.-S. Ahn, Y. Chen, and K. L. Moore, "Iterative learning control: Brief survey and categorization," *IEEE Trans. Syst., Man, Cybern. C*, vol. 37, no. 6, pp. 1099–1121, Nov. 2007.
 [9] D. Shen and Y. Wang, "Survey on stochastic iterative learning control," *J. Process Control*, vol. 24, no. 12, pp. 64–77, 2014.
 [10] D. Shen and X. Li, "A survey on iterative learning control with randomly varying trial lengths: Model, synthesis, and convergence analysis," *Annu. Rev. Control*, vol. 48, pp. 89–102, 2019.
 [11] T. Seel, C. Werner, J. Raisch, and T. Schauer, "Iterative learning control of a drop foot neuroprosthesis - generating physiological foot motion in paretic gait by automatic feedback control," *Control Eng. Pract.*, vol. 48, pp. 87–97, 2016.
 [12] M. Guth, T. Seel, and J. Raisch, "Iterative learning control with variable pass length applied to trajectory tracking on a crane with output constraints," in *Proc. 52nd IEEE Conf. Decis. Control*, Dec. 2013, pp. 6676–6681.
 [13] D. Shen, W. Zhang, Y. Wang, and C. Chien, "On almost sure and mean square convergence of P-type ILC under randomly varying iteration lengths," *Automatica*, vol. 63, pp. 359–365, 2016.
 [14] T. Seel, T. Schauer, and J. Raisch, "Monotonic convergence of iterative learning control systems with variable pass length," *Int. J. Control*, vol. 90, no. 3, pp. 393–406, 2017.
 [15] D. Meng and J. Zhang, "Deterministic convergence for learning control systems over iteration-dependent tracking intervals," *IEEE Trans. Neural Netw. Learn. Syst.*, vol. 29, no. 8, pp. 3885–3892, Aug. 2018.
 [16] X. Li, J.-X. Xu, and D. Huang, "An iterative learning control approach for linear systems with randomly varying trial lengths," *IEEE Trans. Autom. Control*, vol. 59, no. 7, pp. 1954–1960, Jul. 2014.
 [17] X. Li and D. Shen, "Two novel iterative learning control schemes for systems with randomly varying trial lengths," *Syst. Control Lett.*, vol. 107, pp. 9–16, 2017.
 [18] X. Li, J.-X. Xu, and D. Huang, "Iterative learning control for nonlinear dynamic systems with randomly varying trial lengths," *Int. J. Adapt. Control Signal Process.*, vol. 29, no. 11, pp. 1341–1353, 2015.
 [19] J. Shi, J. Xu, J. Sun, and Y. Yang, "Iterative learning control for time-varying systems subject to variable pass lengths: Application to robot manipulators," *IEEE Trans. Ind. Electron.*, vol. 67, no. 10, pp. 8629–8637, Oct. 2020.
 [20] X. Jin, "Iterative learning control for MIMO nonlinear systems with iteration-varying trial lengths using modified composite energy function analysis," *IEEE Trans. Cybern.*, vol. 51, no. 12, pp. 6080–6090, 2021.
 [21] N. Lin, R. H. Chi, and B. Huang, "Auxiliary predictive compensation-based ilc for variable pass lengths," *IEEE Trans. Syst. Man Cybern. Syst.*, vol. 51, no. 7, pp. 4048–4056, Jul. 2021.
 [22] N. Amann, D. H. Owens, and E. Rogers, "Iterative learning control using optimal feedback and feedforward actions," *Int. J. Control*, vol. 65, no. 2, pp. 277–293, 1996.
 [23] K. L. Barton and A. G. Alleyne, "A norm optimal approach to time-varying ILC with application to a multi-axis robotic testbed," *IEEE Trans. Control Syst. Technol.*, vol. 19, no. 1, pp. 166–180, Jan. 2011.
 [24] B. Chu and D. H. Owens, "Accelerated norm-optimal iterative learning control algorithms using successive projection," *Int. J. Control*, vol. 82, no. 8, pp. 1469–1484, 2009.
 [25] Y. Chen, B. Chu, and C. T. Freeman, "Generalized iterative learning control using successive projection: Algorithm, Convergence, and Experimental Verification," *IEEE Trans. Control Syst. Technol.*, vol. 28, no. 6, pp. 2079–2091, Nov. 2020.
 [26] S. Tarbouriech, G. Garcia, and A. H. Glattfelder, *Advanced Strategies in Control Systems with Input and Output Constraints*. Springer, 2007.
 [27] Y. Liu, Y. N. Wang, Y. F. Mei, and Y. L. Wu, "Boundary iterative learning control of a flexible riser with input saturation and output constraint," *IEEE Trans. Syst. Man Cybern. Syst.*, vol. 52, no. 11, pp. 7044–7052, Nov. 2022.
 [28] J. H. Lee, K. S. Lee, and W. C. Kim, "Model-based iterative learning control with a quadratic criterion for time-varying linear systems," *Int. J. Control*, vol. 36, no. 5, pp. 641–657, 2000.
 [29] B. Chu and D. H. Owens, "Iterative learning control for constrained linear systems," *Int. J. Control*, vol. 83, no. 7, pp. 1397–1413, 2010.
 [30] P. Janssens, G. Pipeleers, and J. Swevers, "A data-driven constrained norm-optimal iterative learning control framework for LTI systems,"

- IEEE Trans. Control Syst. Technol.*, vol. 21, no. 2, pp. 546–551, Mar. 2013.
- [31] R. Chi, X. Liu, R. Zhang, Z. Hou, and B. Huang, “Constrained data-driven optimal iterative learning control,” *J. Process Control*, vol. 55, pp. 10–29, 2017.
- [32] S. Mishra, U. Topcu, and M. Tomizuka, “Optimization-based constrained iterative learning control,” *IEEE Trans. Control Syst. Technol.*, vol. 19, no. 6, pp. 1613–1621, Nov. 2011.
- [33] C. T. Freeman and Y. Tan, “Iterative learning control with mixed constraints for point-to-point tracking,” *IEEE Trans. Control Syst. Technol.*, vol. 21, no. 3, pp. 604–616, May 2013.
- [34] A. Haber, R. Fraanje, and M. Verhaegen, “Linear computational complexity design of constrained optimal ILC,” in *Proc. 50th IEEE Conf. Decision and Control and European Control Conf.*, Orlando, FL, USA, 2011, pp. 5343–5348.
- [35] X. Yu, Z. Hou, and M. M. Polycarpou, “A data-driven ILC framework for a class of nonlinear discrete-time systems,” *IEEE Trans. Cybern.*, vol. 52, no. 7, pp. 6143–6157, 2022.
- [36] T. Glück, M. Blank, D. Büchl, and A. Kugi, “Convex constrained iterative learning control using projection: Application to a smart power switch,” *IEEE Trans. Control Syst. Technol.*, vol. 26, no. 5, pp. 1818–1825, 2018.
- [37] Y. Guo and S. Mishra, “Constrained optimal iterative learning control with mixed-norm cost functions,” *Mechatronics*, vol. 43, pp. 56–65, 2017.
- [38] H. Tao, W. Paszke, E. Rogers, K. Gałkowski, and H. Yang, “Modified newton method based iterative learning control design for discrete nonlinear systems with constraints,” *Syst. Control Lett.*, vol. 118, pp. 35–43, 2018.
- [39] J. Lu, Z. Cao, Q. Hu, Z. Xu, W. Du, and F. Gao, “Optimal iterative learning control for batch processes in the presence of time-varying dynamics,” *IEEE Trans. Syst. Man Cybern. Syst.*, vol. 52, no. 1, pp. 680–692, 2022.
- [40] H. Tao, J. Li, Y. Chen, V. Stojanovic, and H. Yang, “Robust point-to-point iterative learning control with trial-varying initial conditions,” *IET Control Theory Appl.*, vol. 14, no. 19, pp. 3344–3350, 2020.
- [41] S. J. Wright, *Primal-dual interior-point methods*. SIAM, 1997.
- [42] E. A. Yildirim and S. J. Wright, “Warm-start strategies in interior-point methods for linear programming,” *SIAM J. Optim.*, vol. 12, no. 3, pp. 782–810, 2002.
- [43] D. Wang, M. Ha, and M. Zhao, “The intelligent critic framework for advanced optimal control,” *Artif. Intell. Rev.*, vol. 55, no. 1, pp. 1–22, 2022.
- [44] D. Wang, J. Qiao, and L. Cheng, “An approximate neuro-optimal solution of discounted guaranteed cost control design,” *IEEE Trans. Cybern.*, vol. 52, no. 1, pp. 77–86, 2022.
- [45] M. Poot, J. Portegies, and T. Oomen, “On the role of models in learning control: Actor-critic iterative learning control,” *IFAC-PapersOnLine*, vol. 53, no. 2, pp. 1450–1455, 2020.
- [46] M. Meindl, D. Lehmann, and T. Seel, “Bridging reinforcement learning and iterative learning control: Autonomous motion learning for unknown, nonlinear dynamics,” *Front. Robot. AI*, vol. 9, 2022.
- [47] J. Nocedal and S. J. Wright, *Numerical Optimization*, 2nd ed. New York, NY: Springer, 2006.
- [48] Q.-Y. Xu and X.-D. Li, “Adaptive fuzzy ILC of nonlinear discrete-time systems with unknown dead zones and control directions,” *Int. J. Syst. Sci.*, vol. 49, no. 9, pp. 1878–1894, 2018.
- [49] C.-J. Chien, “A combined adaptive law for fuzzy iterative learning control of nonlinear systems with varying control tasks,” *IEEE Trans. Fuzzy Syst.*, vol. 16, no. 1, pp. 40–51, 2008.
- [50] M. A. Balootaki, H. Rahmani, H. Moeinkhah, and A. Mohammadzadeh, “On the synchronization and stabilization of fractional-order chaotic systems: Recent advances and future perspectives,” *Phys. A, Stat. Mech. Appl.*, vol. 551, p. 124203, 2020.
- [51] A. Mohammadzadeh and T. Kumbasar, “A new fractional-order general type-2 fuzzy predictive control system and its application for glucose level regulation,” *Appl. Soft Comput.*, vol. 91, p. 106241, 2020.
- [52] A. Mohammadzadeh, M. H. Sabzalian, and W. Zhang, “An interval type-3 fuzzy system and a new online fractional-order learning algorithm: Theory and practice,” *IEEE Trans. Fuzzy Syst.*, vol. 28, no. 9, pp. 1940–1950, 2020.
- [53] A. Mohammadzadeh, O. Castillo, S. S. Band, and A. Mosavi, “A novel fractional-order multiple-model type-3 fuzzy control for nonlinear systems with unmodeled dynamics,” *Int. J. Fuzzy Syst.*, vol. 23, no. 6, pp. 1633–1651, 2021.
- [54] K. Watanabe, J. Tang, M. Nakamura, S. Koga, and T. Fukuda, “A fuzzy-gaussian neural network and its application to mobile robot control,” *IEEE Trans. Control Syst. Technol.*, vol. 4, no. 2, pp. 193–199, Mar. 1996.